EPSC Abstracts
Vol. 5, EPSC2010-212, 2010
European Planetary Science Congress 2010

Solar Wind influences on Critical Behavior of the Terrestrial Magnetosphere

J. Wanliss (1), V. Uritsky (2) and J. Weygand (3)
(1) Presbyterian College, South Carolina, USA, (2) University of Calgary, Canada, (3), University of California, Los Angeles, USA, (jawanliss@presby.edu / Fax: + 1-864-833-8993)

Abstract

Spatiotemporal activity in the high-latitude terrestrial magnetosphere exhibits signatures of self-organized criticality (SOC), a robust multiscale stochastic regime observed in driven nonlinear systems with many coupled degrees of freedom. Here, we examine signatures of avalanching and multiscale behavior in the dynamics of geomagnetic disturbances at low-latitudes, and compare these with the solar wind driver. We examine the burst lifetime distribution functions of solar wind coupling functions over solar minimum and maximum and find clear power-law exponents for different activity thresholds. Ensemble average dynamics of activity bursts in the low-latitude fluctuations are scale-free and are characterized by consistent values of critical spreading scaling exponents. This suggests that the inner magnetosphere operates in a nonequilibrium critical state possibly associated with SOC-like conditions in the solar–terrestrial system.

1. Introduction

Although physical mechanisms of individual activity bursts in the inner magnetosphere have been investigated in numerous case studies, little is known about ensemble-averaged statistical properties of these events. The necessity of such statistical analysis is rooted in the fact that in general, nonlinear systems with multiple spatially distributed sources of instability cannot be completely characterized in deterministic terms. A significant portion of information on the dynamics of such systems, which can be extracted by appropriate statistical-physical methods of analysis, is contained in multiscale correlations of non-Gaussian random variables.

Magnetospheric indices such as AE (auroral electrojet) have proven useful to elucidate statistical and other properties of the solar wind-magnetosphere interaction [1-4]. Freeman et al. [4] examined the AE indices to test for evidence that the magnetosphere is a self-organized and critical system. Since a component of the AE indices is strongly related to the solar wind driving function VBs [5], where V is the solar wind speed and Bs is the rectified southward interplanetary magnetic field (IMF) component, they considered the possibility that the solar wind, rather than the magnetosphere, was the source of the scale-free properties. They found that the scale-free properties of the index very closely followed the scale-free properties of the solar wind, namely the ε-parameter, related to solar wind power. This indicated the possibility that the scale-free properties of AE had their origin in the solar wind. Uritsky et al. [3] demonstrated that the activity bursts in AE and solar wind fluctuations have different dynamical critical scaling features and therefore asserted that the solar wind cannot be responsible for the critical behavior of the magnetosphere on timescales shorter than 3.5 hours.

Here we follow the analysis of Freeman et al. [4], but for the SYM-H index rather than the high-latitude AE indices. SYM-H is a global low-latitude index, mainly related to magnetospheric fluctuations in the ring current. We examine the scale-free burst lifetime distributions of SYM-H and compare them to the distributions from contemporaneous solar wind observations. This provides opportunity to evaluate the extent to which scale-free properties of the SYM-H burst lifetime distributions originate in solar wind rather than directly via inner magnetospheric processes – those responsible for the bulk of the SYM-H fluctuations.

Another way to test for critical behavior is examination of so-called dynamic critical scaling exponents. Critical behavior in equilibrium systems is characterized by the propagation of long-range correlations through the system through fine-tuning of a control parameter. This shows that near the critical point, various systems tend to produce long-range scale-free correlations with universal statistical properties. The most familiar setting for discussion of critical system reconfigurations is phase transitions found in thermodynamic equilibrium.

Dickman [6] and Muñoz et al. [7] developed a theory to characterize dynamical properties of critical

reconfigurations – the so-called avalanches [8] – occurring in a general class of nonlinear systems with many coupled degrees of freedom. It has been predicted that if N(τ) is the average number of active avalanche sites (average area of excitation in the continuum limit), where τ is the delay time measured from the initiation of each avalanche, then close to the critical point, and for delay times less than the time-scale introduced by finite-size effects, Similarly, if Ps(τ) is the probability that an avalanche survives by this time, then The power law exponents η and δ are called spreading-exponents [7]. One can also measure the size S of each avalanche, which is the total number of active sites contributing to the reconfiguration, and its lifetime T. In a nonequilibrium critical state such as SOC, there exists a relationship between the avalanche size and avalanche lifetime. Using the definition of and , it is easy to show that the average number of active site in the surviving runs which produced avalanches with scales as . The characteristic size of the event described by this lifetime is given by the time integral of this quantity, and therefore (see [7] for more details). Scaling laws similar to this expression are called scaling relations and play a central part in quantitative analysis of nonequilibrium critical systems [6].

2. Analysis

In a physical system the time interval between two "events" is called a waiting-time, for instance, the time between avalanches. Various definitions could be used, for example the time interval between event triggering [*9*], the time interval between maxima in intensity [*10*], the time interval from the end of a burst and the start of the next one [*11*], or the time interval when intensity fluctuations are above a given intensity [*3*]. We will label these respectively as the waiting-times, the interpeak, quiet, and burst lifetimes. If there is a lack of a characteristic time scale the probability densities vary with power law relations

$$P(\tau) \sim \tau^{-\gamma}$$

where γ is the scaling constant, and τ is the time length during which fluctuations follow one of the above time scale definitions. In this paper we consider the *burst lifetimes* with constant thresholds as defined by *Freeman et al.* [3]. A constant threshold may be used since if the system producing the signal is in a SOC state the gradient of the power-law *portion* of the burst lifetime distribution will be independent of the threshold level [*12*]. To properly evaluate the scaling exponent we must adopt an apt condition for the size Δ_i of the *i*th bin. Since we expect the burst lifetime distribution to be an inverse power law, bins of equal size will result in those corresponding to large times to collect only a small amount of data, resulting in an unbalanced weight and unreliable calculation of the power law exponent. For this reason $P(\tau)$ was calculated by adopting bin sizes that are equal in logarithm space. That is, $ln(\tau_i)$-$ln(\tau_{i-1})$ is constant, where τ_i and τ_{i-1} are the centers of consecutive bins. The size of the *i*th bin, $\Delta_i = \tau_i - \tau_{i-1}$, will compensate for the decrease in the density of the data. The probability density for each bin is given by

$$P(\tau_i) = n_i / N\Delta_i$$

where n_i is the number of data points in the *i*th bin, and N is the total number of lifetimes computed from the original signal $X(t)$.

In this paper $X(t)$={*SYM-H*, *SYM-H**, VB_s, ε, *B*, ρ}, where VB_s is defined above and

$$\varepsilon = 2\times10^7 \cdot VB^2 \sin^4(\theta/2),$$
$$B^2 = B_x^2 + B_y^2 + B_z^2,$$
$$\theta = \tan^{-1}(B_y / B_z),$$

with IMF components B_x, B_y, and B_z in GSM coordinates; ε is expressed in Watts when V is in km/s and B is in nanoTesla , and plasma density ρ is in m^{-3}. Solar wind data were interpolated with 1 minute cadence for comparison with *SYM-H*. A relatively complete record of the solar wind data is available from 1995 onwards. The solar wind records are constructed from available satellite data from solar wind monitors. The key parameter database from the GEOTAIL, WIND, and ACE spacecraft was used to construct this time series on a month-by-month basis. The key parameter database for the above satellites was consulted, and when there was more than one satellite sampling the solar wind, data from the satellite was selected that had the fewest gaps. Here we analyze data around solar minimum (1998) and maximum (2003). The *SYM-H* records are from the World Data Center, Japan.

For each dataset a set of thresholds was compiled that corresponded to the 10, 25, 50, 75, and 90 percentiles of the cumulative probability distribution of the respective series. These thresholds were set to test the original assumption that the power law slopes are threshold independent. The shape of the distributions for VB_s, and ε.

During solar maximum the scaling properties of low-latitude magnetosphere, whose output is recorded by *SYM-H*, is not purely a direct response to the scale-free properties of the solar wind but is due to inherent properties of the inner magnetosphere. This is most clearly seen by Figure 2, summarized in Table 1.

These results are interesting but, as mentioned in the Introduction, we have other avenues also to study critical behavior, for instance the theory of nonequilibrium systems and dynamic critical scaling [6,7].

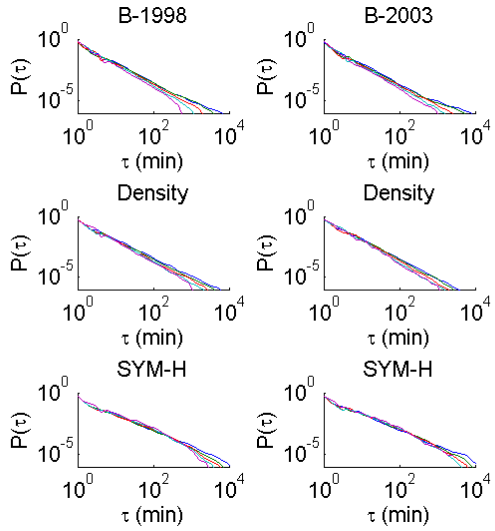

Figure 1: Waiting time distributions, from top to bottom of total magnetic field *B*, number density, *SYM-H*. The left column shows results for solar minimum (1998), and the right column for solar maximum (2003). The percentiles are color coded.

The nonequilibrium theory predicts that if N(τ) is the average number of active avalanche sites (average area of excitation in the continuum limit), where τ is the delay time measured from the initiation of each avalanche, then close to the critical point, and for delay times less than the time-scale introduced by finite-size effects, $N \propto \tau^{\eta}$. Similarly, if $P_s(\tau)$ is the probability that an avalanche survives by this time, then $P_s \propto \tau^{-\delta}$. The power law exponents η and δ are called spreading-exponents [*7*].

Table 1: Scaling exponents obtained from the 50th percentile waiting time distributions.

Parameter	1995-1998	2000-2003
VB_s	*1.30±0.08*	*1.54±0.07*
ε	*1.32±0.09*	*1.59±0.08*
SYM-H	*1.24±0.06*	1.29±0.05

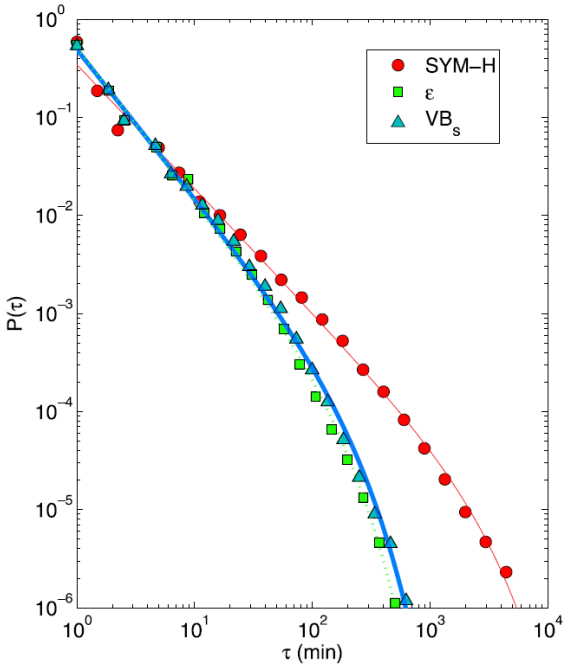

Figure 2: Comparison of the best fit functions for 1995–2005 (colored lines) to the burst lifetime distribution functions for SYM-H (red circles), ε (green squares), and VBs (blue triangles).

One can also measure the size *S* of each avalanche, which is the total number of active sites contributing to the reconfiguration, and its lifetime *T*. In a nonequilibrium critical state such as SOC, there exists a relationship between the avalanche size and avalanche lifetime. Using the definition of δ and η, it is easy to show that the average number of active site in the surviving runs which produced avalanches with $T > \tau$ scales as $\tau^{\eta+\delta}$. The characteristic size

S of the event described by this lifetime is given by the time integral of this quantity, and therefore $S \sim T^{1+\eta+\delta}$ (see [7] for more details). Scaling laws similar to this expression are called scaling relations and play a central part in quantitative analysis of nonequilibrium critical systems.

The best-fit critical scaling exponents, calculated in a least-squares sense, were $\eta = 0.263 \pm 0.008$ and $\delta = 0.416 \pm 0.004$. Solar-wind exponents do not exist in our data set, as there are no scaling regions. When they exist, the dynamic critical exponents can, to some extent, be related theoretically with avalanche scaling exponents. The latter are calculated from the probability distributions of avalanche sizes and lifetimes. We approximated these distributions by power laws with exponential cutoffs

$$P(S) \propto S^{-t_S} \exp(-S/S_c)$$
$$P(T) \propto T^{-t_T} \exp(-T/T_c),$$

The latter account for deviations from self-similar statistics at largest scales which occurs because of the paucity of large space storms with these largest timescales. In Figure 3 we have plotted these distributions for one of the thresholds. Table 2 presents the power law exponents and other fitting parameters calculated by a least squares fit of the probability distributions for all studied thresholds; they were robust irrespective of threshold used.

Table 2: Scaling exponents obtained from the 50th percentile waiting time distributions.

Percentile	t_S	t_T
90	*1.14±0.03*	*1.30±0.04*
50	1.09 ±0.04	1.11 ±0.05
10	1.13 ±0.03	1.26 ±0.03

The best-fit critical exponent calculated of size versus lifetime was 1.705 ± 0.022. As mentioned previously, in critical avalanching systems, the size and lifetimes should be related as $S \propto T^{1+\eta+\delta}$. Again, we have found that the experimentally determined relationship between avalanche size and lifetime is near the theoretical value predicted for this state ($1+\eta+\delta = 1.679 \pm 0.063$).

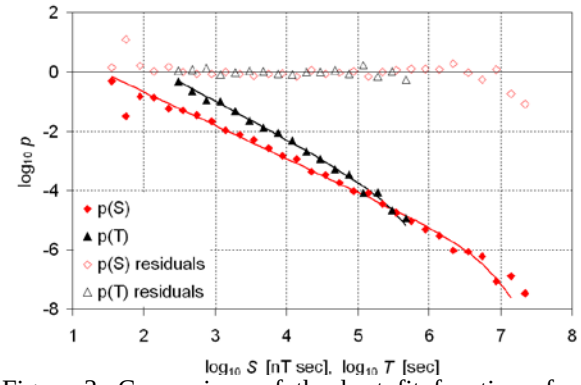

Figure 3: Comparison of the best fit functions for 1995–2005 (colored lines) to the burst lifetime distribution functions for SYM-H (red circles), ε (green squares), and VBs (blue triangles).

6. Summary and Conclusions

The waiting time study finds that *SYM-H* burst lifetime distributions always show power law scaling with a similar scaling exponent during solar minimum and maximum; this is a robust feature suggestive of a SOC generating mechanism. During solar minimum the critical scaling exponents obtained for *SYM-H*, VB_s and ε were essentially the same. However, during solar maximum they were dissimilar. This is a surprising result, since intuitively one might expect more direct coupling of the statistical behavior of *SYM-H* and the solar wind during solar maximum.

For the dynamic critical scaling study we find broad-band scaling in the dynamics of the SYM-H index which is distinct from that in the solar wind drive. Irrespective of its physical interpretation, this observation adds a valuable piece of information to the existing picture of the solar wind–magnetosphere interaction by revealing its multiscale nonlinearity (our statistics show that there are no time scales at which the magnetospheric response is linear). It can also be used for validating existing and future ring current models in terms of their ability to correctly represent the cross-scale coupling effects in this system. The second, so far less solid level of results is our demonstration of the possibility that the multiscale dynamics of the ring current system, as reflected by SYM-H, is a result of its cooperative behavior governed by a specific statistical principle.

Acknowledgements

This material is based upon work supported by the National Science Foundation under Grants No. 0449403 and 0417690. SYM-H data are from WDC-Kyoto. Solar wind data are from CDAWEB. SDG.

References

[1] Uritsky, V.M. and M. I. Pudovkin (1998), Low frequency 1/f-like fluctuations of the AE-index as a possible manifestation of self-organized criticality in the magnetosphere, *Annales Geophysicae*, 16:1580-1588..

[2] Consolini, G., and P. De Michelis (1998), Non-Gaussian distribution function of AE-index fluctuations: Evidence for time intermittency, *Geophys. Res. Lett.*, 25, 4087-4090.

[3] Uritsky, V.M., A. J. Klimas, and D. Vassiliadis (2001b), Comparative study of dynamical critical scaling in the auroral electrojet index versus solar wind fluctuations, *Geophys. Res. Lett.*, 28, 3809-3812.

[4] Freeman, M.P., N. W. Watkins, and D. J. Riley (2000), Evidence for a solar wind origin of the power law burst lifetime distribution of the AE indices, *Geophys. Res. Lett.*, 27, 1087-1090.

[5] Bargatze, L. F., et al. (1985), Magnetospheric impulse response for many levels of magnetosphere activity, *J. Geophys. Res.*, 90, 6387-6394.

[6] Dickman R. (1996), Nonequilibrium Critical Spreading in Two Dimensions, Phys. Rev. E, 53(3), 2223-2230.

[7] Muñoz, M. A., et al. (2001), Sandpiles and absorbing-state phase transitions: recent results and open problems, in "Modeling Complex Systems", Eds. J. Marro and P. L. Garrido, AIP Conference Proceedings, 574, 102.

[8] Bak, P., C. Tang, and K. Wiesenfeld (1988), Self-organized criticality, Phys. Rev. A., 38, 364-374.

[9] Wheatland, M.S. (2000), The origin of the solar-flare waiting-time distribution, Astr. J., L109-L112.

[10] Choe, W., et al. (2002), Nonlinear time series analysis of interpeak intervals of AL data, *J. Geophys. Res.*, 107(A11), 1392, doi:10.1029/2001JA002010.

[11] Sánchez, R., et al. (2002), Quiet- time statistics: A tool to probe the self-organized-criticality systems from within the strong overlapping regime, *Phys. Rev. E*, 66, 036124, doi:10.1103/PhysRevE.66.036124.

[12] Freeman et al., 2000Author, D. and Author, E.: Second example of a cited book, Example Publishing House, 2000.

[13] Paczuski, M., S. Boettcher, and M. Baiesi (2005); Intercurrence times in the Bak-Tang-Wiesenfeld sandpile model: A comparison with the observed statistics of solar flares, *Phys. Rev. Lett.*, 95(18), 181102.